

# CHEMICAL AND STRUCTURAL CHANGES IN POPLAR WOOD UPON STEAM TREATMENT AT CONSTANT TEMPERATURE AND PRESSURE CONDITIONS FOR DIFFERENT TIME INTERVALS

SHARAD RAGHUVANSHI, HINA KHAN, VAISHALI SAROHA, ASHISH KADAM and  
DHARM DUTT

*Department of Paper Technology, Indian Institute of Technology,  
Roorkee, 247667, Uttarakhand, India*

✉ *Corresponding author: D. Dutt, dharm.dutt@pt.iitr.ac.in*

*Received June 29, 2021*

Technology advancement has helped in the development of high-throughput equipment for the analysis of raw material in paper industries. In this research, we have used some advanced techniques to analyze the pore size, structural and chemical changes, and cellulose crystallinity of poplar wood pretreated with steam at constant temperature and pressure conditions for different treatment time. Samples were analyzed by the nitrogen adsorption test, Fourier-transform infrared spectroscopy – attenuated total reflectance (FTIR–ATR), X-ray diffraction (XRD), and field scanning electron microscopy (FE-SEM). Slit-shaped pores were formed, with a diameter of 2.12 nm, after 30 minutes of treatment. FTIR results revealed the degradation of the lignin skeleton through the formation of guaiacyl and syringyl units and deformation in the cellulose and hemicelluloses structure. The crystallinity index (*CI*) increased upon steam treatment for up to 15 min, but after that, a drop in the *CI* was observed. The crystallite thickness ( $d_{200}$ ) increased after 15 min of treatment, due to the rearrangement of cellulose chains. However, a further increase in steam treatment duration to 30 min resulted in a decline of  $d_{200}$ , followed by an increase in the cellulose II crystalline region and  $d_{020}$ . The steam treatment duration of 15-30 min was found to be a critical time interval, which led to increases in the number of mesopores, *CI*,  $d_{200}$ , and the cellulose II region in the poplar wood.

**Keywords:** steam, lignin, cellulose, mesopores, cellulose crystallinity

## INTRODUCTION

Wood is a natural and renewable resource found abundantly on the earth crust and used as a raw material in a variety of industries, from furniture manufacture to construction, fuel, decorative and household items *etc.* The composition of wood is based on three main components, *i.e.* cellulose (~70%), lignin (~20%) and hemicelluloses (~10%). These components are responsible for the cell wall composition. Wood cells are made up of vertical cells, *i.e.*, tracheids or vessel elements and horizontal ray cells joined by pits for the transportation of water. The wood cells consist of the middle lamella, primary wall, S1, S2, and S3 layers, which are made of lignin, hemicelluloses and cellulose. Due to the tough layers of lignin around the middle lamella and primary wall, the porosity is very low, not enough for enzymes or polymeric molecules to penetrate and reach the S1, S2, and

S3 layers.<sup>1,2</sup> Therefore, different pretreatments of wood have been deemed necessary.

Steam treatment has been found to be effective at a high temperature, of 160 °C, causing permeability of gases and moisture, and also resulting in the breakdown of cellulose chains.<sup>3</sup> It has been reported that the breakdown of hemicelluloses also depends on the reaction time and the pressure in the reactor.<sup>4</sup> High temperature favours the degradation of S2 and S3 layers, but the steam at constant temperature degrades only the lignin, pectin layer of the middle lamella, and lignin-hemicellulose cross-links in the primary wall cause an increase in the pore diameter in the cell wall.<sup>5,6</sup>

Previous research has reported that the steam explosion pretreatment of poplar chips at controlled temperature and pressure conditions has improved the cellulase hydrolysis yield.<sup>7</sup> A

possible explanation could be the increase in the number of nanopores in poplar chips due to the removal of the hemicellulose fraction. In other studies, steam explosion treatment of poplar chips at high temperature (190 °C) enhanced the enzyme hydrolysis yield.<sup>8,9</sup> Similarly, when Eucalyptus wood chips were subjected to steam treatment, a decrease in the extractives content was observed due to the partial removal of lignin and hemicelluloses fraction that had occurred during the preceding treatment.<sup>10</sup> These mentioned research works have demonstrated the effectiveness of steam explosion and steam treatment at higher temperature and pressure, but did not examine the effects of such treatments on the porosity and morphological characteristics of the wood chips. Meanwhile, this knowledge is imperative to understand the behaviour of wood and the changes occurring at the molecular level under high temperature and pressure conditions.

In this paper, the steam treatment at constant temperature and pressure conditions was investigated to determine the changes in the porosity, structure, and chemical composition of poplar wood due to the breakdown of the pectin layer, lignin, and hemicelluloses chains. Furthermore, the effect of steam duration on crystallinity was assessed, as in earlier research, it was reported that an increase in crystallinity occurred at high temperatures. Moreover, the physical and chemical behaviour of wood at constant temperature and pressure conditions was also investigated in this research.

## EXPERIMENTAL

### Sample preparation

Wood logs of poplar (*Populus* spp.) were collected from a timber manufacturer, Saharanpur (India). Wood specimens (dimensions: 30 mm (L) × 20 mm (T) × 20 mm (R)) were placed into an automated laboratory autoclave at 120 ± 1 °C and 103.4 kPa pressure (longitudinally) for different time intervals, *i.e.*, 15, 30, 60 and 90 min. Samples were allowed to cool down in the autoclave until the temperature reached room temperature. Samples were stored at equilibrium moisture content close to 11-12% in a glass container at 20 ± 1 °C and relative humidity of 65% for 10 days in a conditioned room.

Treated and untreated samples were cut into small wood sticks (dimensions: 6 mm longitudinally, 2 × 2 mm<sup>2</sup> cross-sectionally) for porosity measurement. The sticks were treated with 80%, 90%, 95% and 100% ethanol for 5 min each to remove residual moisture. Using a microtome, the samples were then sliced to 200 µm thickness in the radial direction for

examination by FE-SEM (TESCAN MIRA 3), operating at 5 kV and 1-10 kx. Samples were prepared as described above and then powdered in a ball-mill (Retsch, Germany) operated (for 15 min) at a frequency of 5 Hz to a final fineness of ~5 µm for X-ray diffractometry and FTIR-ATR (spectra range 4000-800 cm<sup>-1</sup> at a resolution of 4 cm<sup>-1</sup>) studies.

### Nitrogen adsorption test and X-ray diffraction

The nitrogen adsorption test was performed using a surface area analyzer (Autosorb iQ USA) at 77.35 K. Dehydrated samples (each ~1.0 g) were degassed at 80 °C for 12 h under high vacuum conditions (<10<sup>-5</sup> Pa) to remove any moisture or impurities from the samples. The nitrogen adsorption isotherm was obtained using AsiQWin 2.0 Software. The total pore volume ( $V_T$ ) was calculated from the volume of the nitrogen gas adsorbed ( $V_N$ ) at a relative pressure of 0.99. The effects of relative gas pressure on wood samples were neglected for the measurement. The shape of the pores was determined by hysteresis loops. The Brunauer-Emmett-Teller surface area ( $S_{BET}$ ) was calculated from a multi-point BET plot.<sup>11</sup> The pore size distribution was calculated by the Barrett-Joyner-Halenda (BJH) method and the Density Functional Theory (DFT) method.<sup>12,13</sup> The X-ray diffractogram was obtained using XRD (RIGAKU ULTIMA IV) with a Cu-K $\alpha$  radiation source ( $\lambda = 1.5406 \text{ \AA}$ ), operating at 40 kV and 30 mA, with the  $2\theta$  range from 5° to 40° and a scan rate of 4°/min. The crystallinity index ( $CI$ ) was calculated by the peak area method (Eq. 1)<sup>14</sup> and crystallite thickness  $d(hkl)$  was calculated using the Scherrer equation (Eq. 2):<sup>15</sup>

$$CI = \frac{A_c}{A_{c+a}} \times 100 \quad (1)$$

$$d(hkl) = \frac{K\lambda}{\beta \cos \theta} \quad (2)$$

where  $CI$  is the crystallinity index, and  $A_c$  is the area of the crystalline region, and  $A_{c+a}$  is the total area of the amorphous and crystalline region.  $d(hkl)$  is crystallite thickness,  $K$  is the Scherrer constant ( $K = 0.9$ ),  $\lambda$  is the X-ray wavelength,  $\beta$  ( $2\theta$ ) is the peak full width at half of maximum intensity (FWHM) (in radians) obtained by Origin Pro 2019b, when peak fitting was done with the Gaussian function, and  $\theta$  is the angle of diffraction of the peak.

### Statistical analysis

The ANOVA analysis was performed with the data from porosity and  $CI$  analysis, using Graph Pad v9.0 program (GraphPad Software Inc., USA). The statistical least-significance-difference test was carried out to test the significant difference between the mean values of the data obtained for treated and untreated samples, at a confidence limit  $p < 0.05$ . The average value was calculated from triplicates.

## RESULTS AND DISCUSSION

### Nitrogen adsorption test

The nitrogen adsorption isotherm (plotted between volume of gas adsorbed ( $V_N$ ) and relative pressure ( $P/P_0$ )) of untreated wood was intermediate between type II and type IV isotherms, referred to as mesoporous material (2–50 nm), according to the nitrogen adsorption isotherm created by IUPAC (International Union of Pure and Applied Chemistry) (Fig. 1a). The symbols  $S_1$ ,  $S_2$ ,  $S_3$  and  $S_4$  represent the samples at different steam processing times, *i.e.*, 15, 30, 60 and 90 min, respectively. The hysteresis curve showed that the mesopores are of H4 type in untreated wood, of H3 type (slit-shaped) in sample  $S_1$  and of H4 type (narrow slit-shaped) in sample  $S_2$ . After the treatment, the wood samples adsorbed more nitrogen gas. However, an increase in the treatment time to 30 min significantly affected the physio-sorption process. After 30 min, no adsorption of nitrogen gas occurred. It was assumed that the treatment time affected the pores of the wood, which causes an increase in gas permeability into the wood.

The graphs between differential pore volume distributions  $dV(d)$  or  $dV/dD$  and pore diameter

( $D$ ) for untreated and treated wood are plotted in Figure 1 (c, d). The pore size distribution showed a sharp broad peak between 1.5 nm and 3 nm. The untreated sample had slit-shaped pores with a diameter of 3.82 nm ( $>2$  nm). However, when the steam treatment was applied for 15 min, the peak intensities showed a drastic increase in the area of the peaks, indicating an increase in the number of pores, a decrease in the pore size of wood (shifting to microporous), and an increase in surface area (Table 1). Whereas after 30 min of treatment, a noticeable change in the peaks was observed as a broadening of the peak intensities, which suggested a large number of pores with an average pore diameter of 2.12 nm had formed. Therefore, the decrease in the number of micropores appeared as an increase in the number of mesopores with more steam penetration. Thus, the intensities of the peaks of the samples were in the order:  $S_1 > S_2 > \text{Untreated}$ , suggesting the effectiveness of treatment duration (Fig. 1c). However, the steam penetration also clogged the mesopores by condensed water uptake. The pore width ( $W$ ) was increased to 3.38 nm after 15 min of treatment, but later it decreased after 30 min.

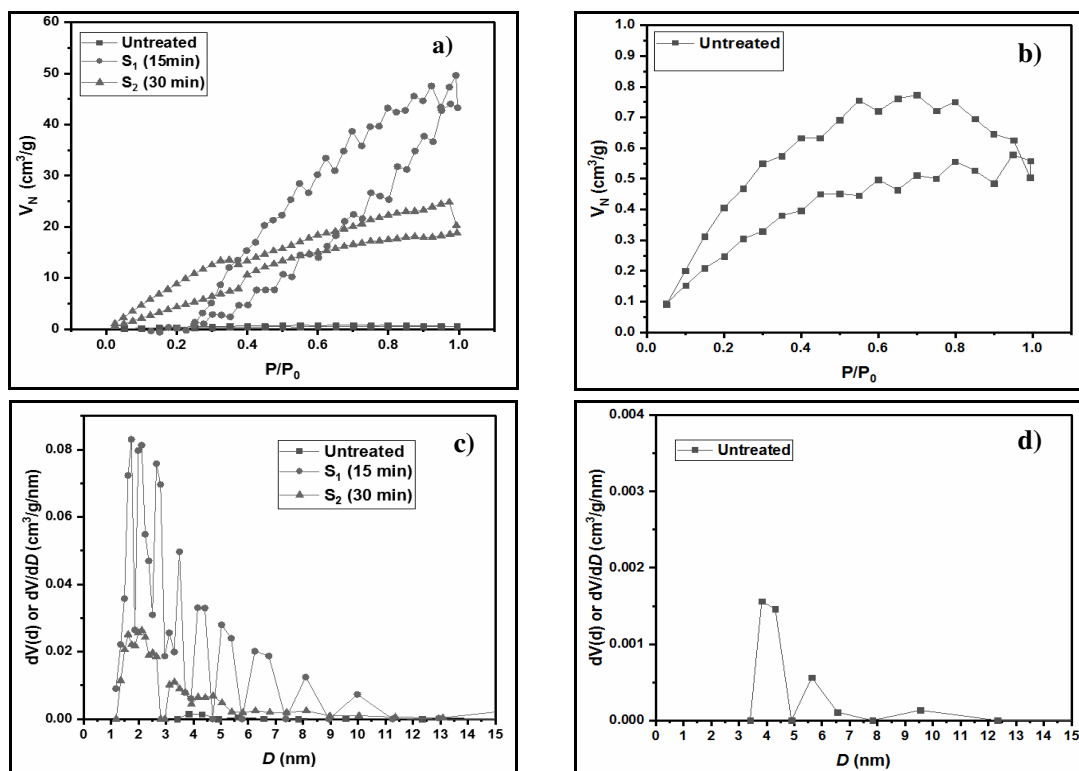


Figure 1: Nitrogen adsorption-desorption isotherm of (a, b) treated and untreated wood; (c, d) pore size distribution of treated and untreated wood

Table 1  
Nitrogen adsorption test results by BET, DFT and BJH methods

| Samples                          | Pore width<br>( <i>W</i> )<br>(DFT)<br>(nm) | Pore volume<br>( <i>V<sub>T</sub></i> )<br>(BJH)<br>(10 <sup>-9</sup> m <sup>3</sup> /g) | Pore diameter<br>( <i>D</i> )<br>(BJH)<br>(nm) | Surface area<br>(SA) (BJH)<br>(m <sup>2</sup> /g) | Specific<br>surface area<br>(SSA <sub>BET</sub> )<br>(m <sup>2</sup> /g) |
|----------------------------------|---|--|--|---|--|
| Untreated                        | 2.76 <sup>a</sup><br>(0.06)                 | 1.01 <sup>a</sup><br>(0.09)  | 3.82 <sup>a</sup><br>(0.03)                    | 0.49 <sup>a</sup><br>(0.01)                       | 1.55 <sup>a</sup><br>(0.04)  |
| S <sub>1</sub>                   | 3.38 <sup>b</sup><br>(0.02)                 | 210 <sup>b</sup><br>(10.0)   | 1.74 <sup>b</sup><br>(0.02)                    | 263.64 <sup>b</sup><br>(0.09)                     | 33.29 <sup>b</sup><br>(0.18)   |
| S <sub>2</sub>                   | 2.18 <sup>c</sup><br>(0.02)                 | 60 <sup>c</sup><br>(0.9)   | 2.12 <sup>c</sup><br>(0.04)                    | 84.60 <sup>c</sup><br>(0.07)                      | 30.20 <sup>c</sup><br>(0.02)   |
| S <sub>3</sub>                   | NA  | NA   | NA   | NA  | NA   |
| S <sub>4</sub>                   | NA  | NA   | NA   | NA  | NA   |
| P value                          | < 0.0001                                    | < 0.0001   | < 0.0001                                       | < 0.0001  | < 0.0001   |
| R <sup>2</sup> value at p < 0.05 | 0.995                                       | 0.994  | 0.999  | 1.0   | 1.0  |

\*NA means no adsorption of nitrogen gas occurred; <sup>a-c</sup> indicate the statistical difference between the sampling positions at p < 0.05; values in brackets are standard deviation

It was assumed that the polysaccharide chains arranged so as to occupy the minimum space

A significant change was observed in the total pore volume (*V<sub>T</sub>*) and BET specific surface area (SSA<sub>BET</sub>) after the steam treatment (Table 1). The *V<sub>T</sub>* and SSA<sub>BET</sub> of the wood cells increased after 15 min of treatment, but were found to reduce after 30 min of treatment. The *V<sub>T</sub>* and SSA<sub>BET</sub> values of untreated wood were 1×10<sup>-9</sup> m<sup>3</sup>/g and 1.55 m<sup>2</sup>/g, respectively. The *V<sub>T</sub>* value of treated wood increased by 210%, while SSA<sub>BET</sub> increased 20-fold after 15 min of treatment. However, the values of *V<sub>T</sub>* and SSA<sub>BET</sub> decreased by 67.9% and 9.28%, respectively, for treated wood after 30 min. The influence of the steam treatment on SSA<sub>BET</sub> was quite similar to that on *V<sub>T</sub>* of the wood. The S<sub>3</sub> and S<sub>4</sub> samples showed a negative adsorption isotherm, meaning that no adsorption of gas occurred on the samples. The possible reasons for this could be the increase in the gaseous permeability, condensed water uptake because of the capillary action in wood cells, and the increase in the number of mesopores.<sup>3</sup>

For the untreated sample, no variation in the features of the pit membrane (PM) was observed (Fig. 2a, 2b). The PM was seen as intact in untreated wood, without any deformation in morphological structure. However, significant deformation in the PM was observed after 15 min and 30 min of treatment because of its rupturing (Fig. 2e, 2f). After 60 min of treatment, the pores on the PM and primary wall (PW) were filled with condensed water (Fig. 2g). The complete rupture of PM, the disappearance of margo (M) and torus (T), and the degradation of secondary

when the pore diameter increased after 30 min of treatment.

cell walls were observed after 90 min of treatment (Fig. 2h). It suggested that the increase in the duration of the steam treatment had an adverse effect on the structure of the cell wall and pore size of the wood, which resulted in fluid and gas permeability in the wood. Subsequently, morphological changes in PM and secondary walls in the wood cells were permanently fixed by further increase in the steam treatment time beyond 30 min.<sup>3</sup>

### Morphological changes

#### Changes in chemical composition

Fourier transform infrared spectroscopy was used to analyze the changes in the chemical composition, by visualizing the peaks of crystalline cellulose at 1316 cm<sup>-1</sup> and 1336 cm<sup>-1</sup> due to the vibrations in CH<sub>2</sub> bonds in crystalline cellulose and hemicelluloses (Fig. 3a). The peak intensities were maximum for the samples treated for 15 min and 90 min, which suggested that the cellulose chains were affected after 15 min of treatment. However, after 30 min, the peak intensity of the CH<sub>2</sub> bands reduced due to a decrease in absorbance, which confirmed the degradation of cellulose and hemicelluloses. The bands at 2840 cm<sup>-1</sup> and 2940 cm<sup>-1</sup> determined the structural, compositional, and crystallinity changes in the treated wood (Fig. 3d).<sup>16</sup> In this case, the crystallinity peak at 2840 cm<sup>-1</sup> and 2940 cm<sup>-1</sup> increased after 15 min of treatment, and variably decreased with further increase in treatment duration.

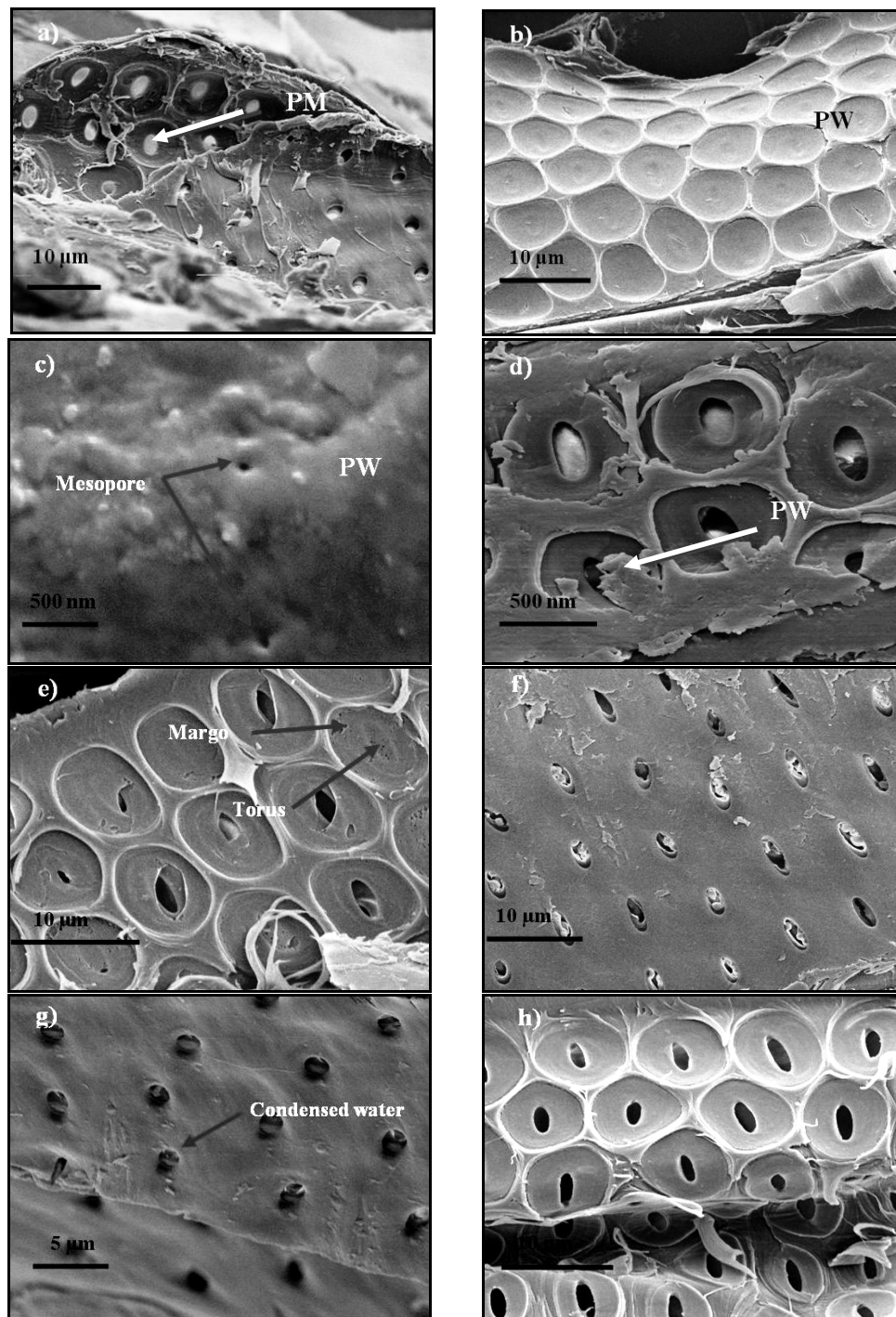


Figure 2: Morphological changes after steam treatment (a, b) untreated wood with intact pit membrane (PM); (c) pores on the primary wall (PW); (d) peel of the primary wall; pit membrane degradation after (e) 15 min; (f) 30 min; (g) 60 min; (h) 90 min

The bands between  $1700\text{ cm}^{-1}$  and  $1750\text{ cm}^{-1}$  reflect the C=O stretching in functional groups (esters, ketones, aldehydes, carbonyls, and carboxylic acids) of lignin and hemicelluloses.<sup>17</sup> This indicated that 15 min of steam treatment

significantly increased the number of C=O bonds in lignin and hemicellulose chains (Fig. 3a). High temperature favours the degradation of lignin and increases the number of C=O bonds.<sup>5</sup> The band at  $1596$  and  $1505\text{ cm}^{-1}$  showed the C=O and C=C

stretch in the benzene ring of the lignin in the following order: 60 min > 15 min > 90 min > 30 min > untreated (0 min), due to the changes in the guaiacyl and syringyl units (Fig. 3c).<sup>17</sup> The degradation of methoxyl groups of the guaiacyl and syringyl units in lignin increased the absorbance peak of the band at 1505 cm<sup>-1</sup>.<sup>5</sup>

The band at 1160 cm<sup>-1</sup> and 1030 cm<sup>-1</sup> showed an increase in signal intensity due to the vibrations in C–O–C bonds of the cellulose and hemicelluloses. This suggested that the steam treatment for 15 min was enough to cause changes in the number of C–O–C bonds, leading to deformation in the cellulose and hemicellulose structure.<sup>18,5</sup>

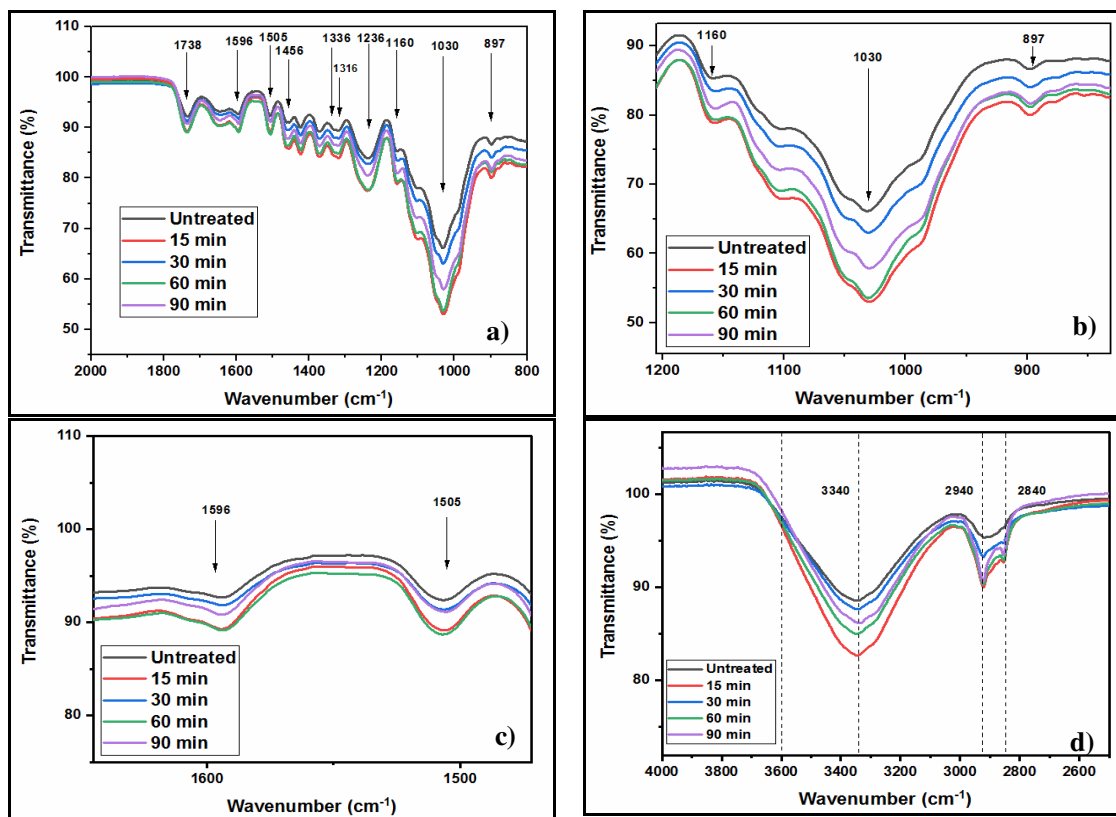


Figure 3: FT-IR spectra (a) treated and untreated wood; (b) cellulose and hemicellulose region 1160-897 cm<sup>-1</sup>; (c, d) lignin skeleton region 1590-1510 cm<sup>-1</sup> and 3300-3600 cm<sup>-1</sup>

Table 2  
Chemical changes occurring upon steam treatment at constant temperature and pressure conditions

| Wavenumber (cm <sup>-1</sup> ) | Chemical changes  | Ref.   |
|--------------------------------|---|--------|
| 1316 and 1336                  | CH <sub>2</sub> wagging vibrations in crystalline cellulose and to OH in-plane bending of amorphous cellulose       | [5]    |
| 1738                           | C=O stretching vibrations in the O=C-OH group of a glucuronic acid unit of xylan                                    | [3,17] |
| 1596                           | C=O stretch of lignin skeleton  | [17]   |
| 1456                           | CH <sub>2</sub> symmetric bending on the xylose ring, xylan backbone  |        |
| 1236                           | C-O stretching in the O=C-O group in xylan  | [5]    |
| 2840 and 2940                  | Symmetric CH <sub>2</sub> stretching and asymmetric CH <sub>2</sub> stretching                                      | [16]   |
| 3340                           | Lignin intra-molecular H-bonds and OH stretching of alcohols and phenols  | [5]    |
| 1030                           | Cellulose and hemicellulose deformation   | [18,5] |
| 1160                           | C–O–C vibrations in cellulose and hemicelluloses  | [18,5] |
| 1505                           | C=C aromatic skeletal vibrations stretching of the benzene ring in lignin   | [23]   |
| 897                            | Deformation of C <sub>1</sub> -H of glucose ring in cellulose and hemicelluloses, β(1-4) glycosidic bonds breakdown | [19]   |

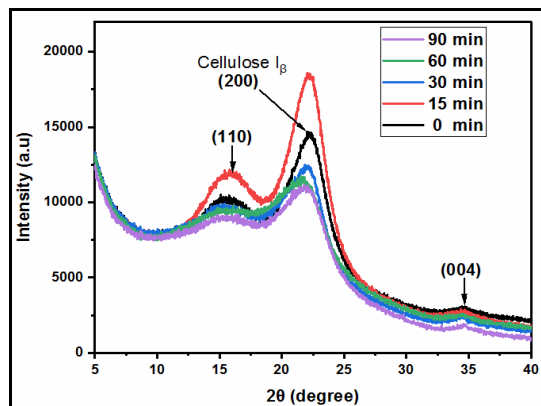


Figure 4: X-ray diffractograms of untreated and steam-treated poplar wood

Cellulose chains began to interact with each other through the C–O–C linkage, which was observed as an increase in the absorption of C–O–C bonds after 15 min. The band at  $897\text{ cm}^{-1}$

Deformation of cellulose at  $897\text{ cm}^{-1}$  can be seen as an increase in the amorphous cellulose and a decrease in cellulose crystallinity.<sup>19</sup> In this case, after 15 min of treatment, the increase in the absorbance peak at  $897\text{ cm}^{-1}$  was observed, which signified an increase in cellulose crystallinity (Fig. 3b). Later, it variably changed with further increase in treatment duration. Table 2 summarizes the chemical changes that occurred during the steam treatment.

#### Changes in cellulose crystalline structure

The structural changes in the cellulose structure after the steam treatment at constant temperature and pressure conditions was studied using X-ray diffractometry. The X-ray diffractograms of treated and untreated wood were plotted in Figure 4. The native form of cellulose found in nature is cellulose  $I_{\beta}$  form, which is common in every wood type. Both crystalline and amorphous cellulose is present in the cell walls of higher plants.<sup>20,21</sup> Cellulose  $I_{\beta}$  has parallel crystalline fibrils chains.<sup>22</sup> In the X-ray diffractogram, the untreated wood samples showed three peaks at  $16.5^{\circ}$ ,  $22.14^{\circ}$ , and  $34.6^{\circ}$ , which correspond to the planes (110), (200), and (004), respectively.<sup>23</sup> The  $2\theta$  angle shift in the plane (200) from  $22.14^{\circ}$  to  $21.8^{\circ}$  corresponds to cellulose II, and the shift to  $20.7^{\circ}$  corresponds to the cellulose III polymorph.

After steam treatment for 15 min, a significant increase in the peak intensity of the planes (200) and (110) was observed. The plane (200) and plane (110) correspond to the diameter of the crystalline cellulose chains. It was suggested that

indicated the glucose ring stretching vibration and deformation in the cellulose structure, with the breakdown of glycosidic bonds.

cellulose and hemicellulose chains were not much negatively affected after 15 min of steam treatment, due to the rearrangement or reordering of cellulose chains in the more crystalline region.<sup>24</sup> However, the plane (004) that corresponds to the length of microfibrils experienced no change after the treatment, which suggested that the length of cellulose chains remained unaffected during the steam treatment up to 90 min.<sup>24</sup>

The crystallinity index ( $CI$ ) was calculated as the area of the crystalline region to the total area (amorphous region + crystalline region). Crystallinity changes were observed in the treated wood. With respect to the data given in Table 3, the  $CI$  of treated wood increased by 0.65% after 15 min of treatment. However, further increase in the treatment time resulted in a reduction of the  $CI$  by 2.9% for 30 min, 3.81% for 60 min, and 5.39% for 90 min, compared to the steam treatment for 15 min.

ANOVA analysis was carried out to investigate the statistical difference between the  $CI$  with the increase in treatment duration. There was a significant difference between the sampling groups at  $p < 0.05$  and a significant influence of treatment time on  $CI$ , as shown in Table 3. The average crystallite size ( $d_{200}$ ) was found to be 2.09 nm for the untreated wood (0 min), while steam treatment significantly affected the average crystallite size (Table 3). The crystallite size ( $d_{200}$ ) was increased in the sample treated for 15 min, but decreased later for 30, 60, and 90 min, with a peak shift to  $21.8^{\circ}$ , which corresponds to the plane (020) of the cellulose II polymorph. The

average crystallite size ( $d_{020}$ ) of the samples treated for 15, 30, and 90 min was calculated as 1.89 nm, 1.52 nm, and 2.05 nm, respectively. The native state of cellulose was not found to be crystalline.<sup>25</sup> Upon increasing the duration of the steam treatment, the cellulose chains begin to organize themselves into a more crystalline

region. However, the continuous increase in steam treatment duration leads to the degradation of cellulose chains, and a shift of the 2 $\theta$  value to the amorphous or semi-crystalline region, which was found to be consistent with the regular decrease of *CI* in samples treated for 30, 60, and 90 min.

Table 3  
Changes in the crystallinity and crystallite size for the different steam processing time

| Processing time (min) | 0                  | 15                 | 30                 | 60                 | 90                  | P value | R <sup>2</sup> value at p < 0.05 |
|-----------------------|--------------------|--------------------|--------------------|--------------------|---------------------|---------|----------------------------------|
| <i>CI</i> (%)         | 81.84 <sup>a</sup> | 82.49 <sup>b</sup> | 79.59 <sup>c</sup> | 78.68 <sup>d</sup> | 77.10 <sup>e</sup>  | <       | 0.995                            |
| (Std. dev.)           | (0.27)             | (0.10)             | (0.11)             | (0.09)             | (0.02)              | 0.0001  |                                  |
| <i>d</i> (nm)         | 2.09 <sup>a</sup>  | 2.15 <sup>a</sup>  | 1.89 <sup>b</sup>  | 1.52 <sup>c</sup>  | 2.05 <sup>a,b</sup> | <       | 0.930                            |
| (Std. dev.)           | (0.06)             | (0.02)             | (0.11)             | (0.04)             | (0.07)              | 0.0001  |                                  |

<sup>a-e</sup> the same letter in the same row indicates no significant difference between the sampling positions at p < 0.05; Std. dev. stands for standard deviation

## CONCLUSION

Steam treatment at constant temperature and pressure conditions affects the mesopore diameter and crystallinity of wood because of the rearrangement in the chemical structure and the cellulose chains. However, as the treatment time increased, the lignin and xylan residues began to degrade. The cellulose crystallinity index increased after 15 min of treatment and then decreased due to the degradation in cellulose chains. Degradation of PM appeared with the increase in the treatment time. However, BET isotherms showed no adsorption of gas in the wood sample treated for more than 30 min. Due to the increase in the mesopore size, the gas and fluid permeability in wood increases, which prevents the physio-sorption of gas. Poplar wood underwent chemical and structural changes after 15 min of steam treatment at constant temperature and pressure, which was reflected in the form of degradation in the lignin skeleton, CH<sub>2</sub> and OH group vibrations in crystalline and amorphous cellulose, and the degradation in the xylan backbone. This research provides a practical understanding of wood behaviour under steam treatment at high temperature and pressure for different duration, employing new high-throughput advanced techniques in paper industries.

**ACKNOWLEDGEMENT:** The authors wish to thank the Ministry of Human Resources and Development, Government of India, for financial support. The authors are thankful to IIT Roorkee

for providing the laboratory and instrumentation facilities.

## REFERENCES

- <sup>1</sup> E. Srebotnik, K. Messner and R. Foisner, *Appl. Environ. Microbiol.*, **54**, 2608 (1988), <https://doi.org/10.1128/aem.54.11.2608-2614.1988>
- <sup>2</sup> C. M. Popescu, C. M. Tibirna, A. L. Manoliu, P. Gradinariu and C. Vasile, *Cellulose Chem. Technol.*, **45**, 565 (2011), [https://www.cellulosechemtechnol.ro/pdf/CCT45.9-10\(2011\)/p.565-569.pdf](https://www.cellulosechemtechnol.ro/pdf/CCT45.9-10(2011)/p.565-569.pdf)
- <sup>3</sup> J. Guo, K. Song, L. Salmén and Y. Yin, *Carbohydr. Polym.*, **115**, 207 (2015), <https://doi.org/10.1016/j.carbpol.2014.08.040>
- <sup>4</sup> N. Jacquet, G. Maniet, C. Vanderghem, F. Delvigne and A. Richel, *Ind. Eng. Chem. Res.*, **54**, 2593 (2015), <https://doi.org/10.1021/ie503151g>
- <sup>5</sup> I. Kubovský, D. Kačíková and F. Kačík, *Polymers*, **12**, 485 (2020), <https://dx.doi.org/10.3390%2Fpolym12020485>
- <sup>6</sup> M. Arshadi and H. Grundberg, in "Handbook of Biofuels Production", edited by R. Luque, J. Campelo and J. Clark, Woodhead Publishing, 2011, pp. 199-220
- <sup>7</sup> H. Wang, Z. Liu, X. Zheng, X. Pan, X. Hui *et al.*, *Carbohydr. Polym.*, **230**, 115622 (2020), <https://doi.org/10.1016/j.carbpol.2019.115622>
- <sup>8</sup> A. Galazka and J. Szadkowski, *Cellulose Chem. Technol.*, **55**, 637 (2021), <https://doi.org/10.35812/CelluloseChemTechnol.2021.55.52>
- <sup>9</sup> Y. Yu, J. Wu, X. Ren, A. Lau, H. Takada *et al.*, *Renew. Sustain. Energ. Rev.*, **154**, 111871 (2022), <https://doi.org/10.1016/j.rser.2021.111871>
- <sup>10</sup> R. Martin-Sampedro, M. E. Eugenio, J. A. Moreno, E. Revilla and J. C. Villar, *Bioresour. Technol.*, **153**, 236 (2014), <https://doi.org/10.1016/j.biortech.2013.11.088>

- <sup>11</sup> S. Brunauer, P. H. Emmett and E. Teller, *J. Am. Chem. Soc.*, **60**, 309 (1938), <https://doi.org/10.1021/ja01269a023>
- <sup>12</sup> E. P. Barrett, L. G. Joyner and P. P. Halenda, *J. Am. Chem. Soc.*, **73**, 373 (1951), <https://doi.org/10.1021/ja01145a126>
- <sup>13</sup> M. Nopens, U. Sazama, S. König, S. Kaschuro, A. Krause *et al.*, *Sci. Rep.*, **10**, 11 (2020), <https://doi.org/10.1038/s41598-020-65066-1>
- <sup>14</sup> E. L. Hult, T. Iversen and J. Sugiyama, *Cellulose*, **10**, 103 (2003), <https://doi.org/10.1023/A:1024080700873>
- <sup>15</sup> J. I. Langford and A. J. C. Wilson, *J. Appl. Crystallogr.*, **11**, 102 (1978), <https://doi.org/10.1107/S0021889878012844>
- <sup>16</sup> I. Spiridon, C. A. Teaca and R. Bodîrlău, *BioResources*, **6**, 400 (2011), <https://doi.org/10.15376/biores.6.1.400-413>
- <sup>17</sup> B. Esteves, A. V. Marques, I. Domingos and H. Pereira, *Maderas Cienc. Tecnol.*, **15**, 245 (2013), <https://dx.doi.org/10.4067/S0718-221X2013005000020>
- <sup>18</sup> W. Peng, L. Wang, M. Ohkoshi and M. Zhang, *Cellulose Chem. Technol.*, **49**, 756 (2015), [https://www.cellulosechemtechnol.ro/pdf/CCT9-10\(2015\)/p.756-764.pdf](https://www.cellulosechemtechnol.ro/pdf/CCT9-10(2015)/p.756-764.pdf)
- <sup>19</sup> M. Akerholm, B. Hinterstoisser and L. Salmén, *Carbohydr. Res.*, **339**, 569 (2004), <https://doi.org/10.1016/j.carres.2003.11.012>
- <sup>20</sup> K. Ruel, Y. Nishiyama and J. P. Joseleau, *Plant Sci.*, **193**, 48 (2012), <https://doi.org/10.1016/j.plantsci.2012.05.008>
- <sup>21</sup> H. Khan, A. Kadam and D. Dutt, *Carbohydr. Polym.*, **229**, 115513 (2020), <https://doi.org/10.1016/j.carbpol.2019.115513>
- <sup>22</sup> M. Poletto, V. Pistor and A. J. Zattera, in “Cellulose – Fundamental Aspects”, edited by T. G. M. Van De Ven, IntechOpen, 2013, pp. 45-68
- <sup>23</sup> W. S. Chen, H. P. Yu, Y. X. Liu, P. Chen, M. X. Zhang *et al.*, *Carbohydr. Polym.*, **83**, 1804 (2011), <https://doi.org/10.1016/j.carbpol.2010.10.040>
- <sup>24</sup> J. Guo, H. Rennhofer, Y. Yin and H. C. Lichtenegger, *Cellulose*, **23**, 2325 (2016), <https://doi.org/10.1007/s10570-016-0982-2>
- <sup>25</sup> U. P. Agarwal, S. A. Ralph, R. S. Reiner and C. Baez, *Cellulose*, **23**, 125 (2016), <https://doi.org/10.1007/s10570-015-0788-7>